Laser Ignition of Single Cylinder Engine and Effects of Ignition Location

Article *in* SAE Technical Papers · April 2013

DOI: 10.4271/2013-01-1631

CITATIONS
18

READS
6,141

2 authors:

Dhananjay Srivastava
Indian Institute of Technology Kharagpur
52 PUBLICATIONS **1,717** CITATIONS

SEE PROFILE

Avinash Kumar Agarwal
Indian Institute of Technology Kanpur
582 PUBLICATIONS **23,244** CITATIONS

SEE PROFILE

SAE International

Laser Ignition of Single Cylinder Engine and Effects of Ignition Location

2013-01-1631
Published
04/08/2013

Dhananjay Srivastava
Indian Institute of Technology - Kanpur

Avinash Kumar Agarwal
I I T Kanpur

doi:10.4271/2013-01-1631

ABSTRACT

Laser is emerging as a strong contender as an alternative ignition source for internal combustion (IC) engines. Short laser pulses of few nanoseconds duration delivered by a Q-switched laser are focused by a lens inside the engine cylinder containing combustible fuel-air mixture. If the peak intensity at the focal point exceeds threshold intensity level, breakdown of combustible gases occurs, which leads to plasma formation. If the energy of the spark generated by plasma is high enough, the mixture ignites. In this investigation, laser ignition (LI) was performed in a single cylinder engine at constant speed and wide open throttle conditions using CNG as fuel. Combustion behavior was recorded using a high speed data acquisition system. For laser ignition of the engine, a laser spark plug was designed and manufactured. Laser spark plug consists of combination of lenses and optical windows. The position of plasma was varied inside the combustion chamber and performance, emissions and combustion characteristics were evaluated at different conditions. A comparative study of combustion with laser ignition and conventional spark plug ignition is also reported.

INTRODUCTION

Stringent exhaust emissions norms and demand of high thermal efficiency can be achieved by ignition of lean air-fuel mixtures in IC engines. However, lean combustion is associated with slower flame propagation speeds, reduced power output and struggle with emissions standards due to complex lean NOx after-treatment. Engine power output can be improved by increasing initial in-cylinder pressure by turbocharging. Increased in-cylinder pressure however requires high secondary voltage to breakdown the gases and initiates the combustion in a spark ignition (SI) engine using conventional spark Ignition system. The amount of energy released between the spark electrodes depends mainly on the pressure inside the combustion chamber at the time of ignition (towards the end of compression stroke) and the distance between these electrodes. An increase in the in-cylinder pressure keeping the same electrode distance would require increased secondary coil voltage applied to the spark plug, which would lead to erosion of electrodes over time. Flame propagation speed in lean mixtures can be increased either by optimizing the position of the ignition point inside the combustion chamber or by multipoint ignition [1, 2, 3]. However point of ignition remains always close to the top of the combustion chamber in a SI engine and cannot be varied too much from this location. These limitations of conventional ignition systems can be overcome by a durable high-energy, electrode-less ignition system, which also has flexibility in terms of spark location, such as laser ignition (LI) system.

When a laser pulse is focused to a sufficiently small spot size, a bright spot appears at the focal point due to breakdown of the surrounding gases [4, 5, 6, 7]. There are four different mechanisms by which laser light can interact with a combustible mixture to generate plasma: (a) Thermal initiation, (b) Photochemical ignition, (c) Resonant ignition, and (d) Non-resonant ignition [8]. Non-resonant breakdown of gases is more favorable in engine applications because it does not require a close match between the laser wavelength and the target gas molecules [9]. In this experimental investigation, LI was achieved through non-resonant mechanism.

In non-resonant ignition, laser beam is tightly focused to a sufficiently small spot to create very high energy density at that focal point. If the energy density is above the critical value, ($>10^{11}$W/cm^2 in air at standard conditions), then localized plasma is generated with temperature of the order of 106 K and pressure of the order of 10^2 MPa [10, 11, 12]. This process is associated with a sharp acoustic sound. Multi-photon ionization and cascade ionization are two generally accepted mechanisms, which lead to breakdown of gases in non-resonant ignition [13]. Multi-photon ionization (MPI) involves simultaneous absorption of number of photons required to achieve the ionization potential of the atoms. Electron librated by the MPI process radially absorb the laser radiations through electron-neutral inverse bremsstralhung collisions (IB). If the gained energy is slightly higher than the ionization potential of the gas, then electrons may ionize an atom by collision, thus producing two electrons of lower energy. These electrons are then available for the process to be repeated, leading to electron avalanche and breakdown of the gases. It is important to note that cascade ionization process requires two necessary conditions for the breakdown of gases. First condition is that a free electron must be present in the focal volume and second condition is that electron must gain energy from the radiation of laser, which is greater than the potential energy of the gas [12]. However, laser near the infrared region has photon energy of approximately 1 eV, whereas ionization potential energy of most gases is more than 10 eV [12]. The possibility of finding free electrons or excited atoms due to natural causes such as local radioactivity, passage of ultraviolet and cosmic ray at the earth's surface is negligible. Tozer [14] pointed out that these are generated at earth's surface at a rate of 10^{-3} cm^{-3} sec^{-1}. Thus laser light itself generates free electrons either from multi-photon ionization or thermionic emissions of impurities and/ or aerosols present in the gas [13].

There are several advantages of LI compared to conventional SI system. Advantages of LI were reviewed by Paul [15]. LI system is electrode-free, therefore there is no erosion effect which is observed in a conventional spark plug system. Thus, the life span of LI system is expected to be significantly longer than the conventional spark plug system. A diode pumped LI system has potential lifetime up to 10,000 h compared to spark plug lifetime of the order of 1000 h [16]. Further, ignition timing as well as the ignition energy and pulse energy deposition rate can be easily controlled in LI [17]. One of the main advantages of LI is that plasma location can be at an optimum position inside the combustion chamber. This way, combustion duration can be reduced by decreasing the maximum flame propagation distance by moving away the flame kernel from the metallic cylinder head surface, which will therefore reduce the heat loss and promote faster early flame growth. Thus, LI could be beneficial in leancombustion, where slow flame propagation is the main hurdle. This type of combustion is not practically feasible while using conventional spark plug. There are several challenges of LI as well. The cost of LI system is quite high at present. It is expected that upon mass production and further developments in the laser systems dedicated to engine applications, cost of production would come down significantly to enable its use in a commercially practical engine system. Propagation of laser beam from laser head to inside of the combustion chamber remains one of main hurdle in development of practical LI system. Durability of optical window, through which, laser beam is guided into the combustion chamber, remains a huge challenge. Optical window must withstand harsh conditions of high pressures and temperatures prevailing in the combustion chamber. Any carbon deposits on the optical window would reduce the transitivity of laser beam, which might lead to engine misfire. However, window fouling was not observed in the 50 h long testing of the engine in the present study.

For LI, minimum energy required for breakdown of gases in order to initiate combustion remains an important parameter. Several researchers [10, 18, 19, 20, 21, 22] evaluated the dependence of breakdown threshold intensity on cylinder pressure. Phuoc [10] measured the threshold intensity in air, O_2, N_2, H_2 and CH_4 using Nd: YAG laser of 1064 nm and 532 nm wavelength and pulse duration of 5.5 ns. The gas pressure was varied from 0.2 bars to 4 bars. Experimental results showed that the breakdown threshold intensity decreased rapidly as the pressure increased. The dependence of threshold intensity on the pressure was found to be strong at shorter wavelengths and it became weaker at longer wavelengths. The dependence of threshold intensity was expressed as proportion of pressure (p^n). The threshold in hydrogen showed a strong pressure dependence with n = −0.69, while in another gases n is ∼−0.4 at λ = 1064 nm. Bradley et al. [21] measured the threshold intensity in air, lean, and rich iso-octane-air mixtures. The threshold intensity dependence on pressure was found to be $n \sim -0.54$ for air. No significant changes were found in the breakdown threshold between lean and rich mixture of isooctane and air. Thus, breakdown threshold intensity decreased rapidly with increasing gas pressure inside the combustion chamber [10, 21, 23]. The dependence of breakdown threshold intensity on gas pressure in case of LI is completely opposite to the conventional spark plug, where breakdown threshold increases with increasing gas pressure [23].

LI in an engine was first demonstrated in 1978 by Dale et al. [24]. A CO_2 laser operating at 10.6 μm with pulse duration of 300 ns was used as an ignition source. With LI, lean limit of air-fuel ratio was extended from 22.5:1 to 27.8:1 and improvement in brake specific fuel consumption (bsfc) was also observed. Biruduganti et al. [25] compared the performance of LI and conventional SI on a single cylinder natural gas engine. Results showed that fuel conversion efficiency for both ignition systems was very close to a maximum of 22.5%. Rate of pressure rise and heat release were higher for LI than SI. NOx emissions were also found to

be higher for LI than SI for all ignition timings, except for very retarded timings. They concluded that LI showed superior combustion than SI due to higher peak in-cylinder pressure, faster burn rates and improved heat release under identical engine operating conditions. Herdin et al. [23] presented the LI of large-bore natural gas engine and reported that the energy required for producing plasma decreases with increasing in-cylinder pressure. Therefore higher charge density in the combustion chamber is favorable condition for LI. McMillian et al. [26] reported that with LI system, total operating envelope of the engine, defined as the area between knock and misfire limit, increases by 46% compared to conventional SI system. NOx emissions in the engine exhaust were also found to be lower from engine with LI system compared to the one with SI system [27, 28, 29] however the test matrix was different. Lower NOx emissions were obtained by Bihari et al. [27] in an engine operating with leaner mixture using LI, while it was still maintaining the same efficiency.

Propagation of laser beam from laser head to inside the combustion chamber is one of hurdle in development of a practical LI system. Bihari et al. [27] proposed two schemes for propagation of laser beam. The first approach was one laser per cylinder scheme, which included a small laser being mounted on each cylinder head. In the second approach; output of a single laser is multiplexed to deliver laser pulses to each cylinder thorough an optical fiber. McIntyre et al. [30] and Kroupa et al. [31] developed a miniature diode pumped Q-switched Nd: YAG laser for LI. Propagation of high power laser through optical fiber still remains a major technical issue. However, hollow core fibers are potential candidates for propagation of laser pulses inspite of high radial losses associated with hollow core fiber [32, 33, 34].

EXPERIMENTAL SET-UP

All experiments were performed in a single cylinder engine. The engine was modified from a production grade diesel engine and was converted to a SI engine in order to introduce greater flexibility for conducting LI/ SI experiments. It is difficult to have flexibility required for conducting these experiments in a production grade engine such as variable spark timings and variable air-fuel ratio (lambda). It is also difficult to modify a cylinder head of a production grade SI engine to accommodate the laser spark plug and pressure transducer because its already quite crowded. Therefore a single cylinder diesel engine (Kirloskar, India; DM-10) was chosen to be modified for use in this investigation because of ease of modifications and its robustness. For converting a production grade diesel engine into a SI engine, several modifications were done. Provision for fuel introduction, spark plug installation and throttling were done. Since, compression ratio (CR) of a diesel engine is relatively higher compared to a typical SI engine therefore CR was reduced by machining the piston. The compression ratio of the engine was reduced from 17.2 (corresponding to a diesel engine) to 10 (Corresponding to a CNG fuelled SI engine). Detailed technical specifications of the test engine are given in table 1.

Table 1. Technical specifications of the test engine

Displaced volume	948 cc
Stroke	116 mm
Bore	102 mm
Connecting rod	232 mm
Compression ratio	10:1
Number of valves	2
Exhaust valve open	35.5° BBDC
Exhaust valve close	4.5° ATDC
Inlet calve open	4.5° BTDC
Inlet calve close	35.5° ABDC

Modified test engine was coupled with an eddy current dynamometer (Accurate Engineering Systems, India; EC50). Engine load indicator, speed indicator, and temperature indicators were mounted on the dynamometer controller panel. Dynamometer was connected to a 3φ A/C motor through a gear box, which may be engaged to start the engine and it gets disconnected, once the engine starts. Air-fuel ratio was controlled by measuring the air flow rate and fuel flow rate separately. Air flow in the intake manifold remains pulsating in nature in a single cylinder engine therefore its accurate measurement is challenging. In order to measure the air flow rate accurately, a large volume air drum (with air pulsation damper) is connected to the air intake manifold. A laminar flow element (LFE) (Meriam, USA; 50MC2-2F) was installed for intake air flow rate measurement into the drum's intake. LFE is connected to a precision manometer, which measures the pressure drop across the orifice plate of the LFE, thus giving the air flow rate measurement accurately. CNG mass flow rate was measured by Coriolis force based fuel flow meter (Emerson, India; CMF010M). A coriolis flow meter comprises of two main components, a sensor (primary element) and a transmitter (secondary element). Coriolis meter infers the gas mass flow rate by sensing the Coriolis force on the vibrating tubes. As the gas flows through vibrating tubes, a phase shift is generated in the signals sensed by sensing coil due to the Coriolis force experiences. The phase shift measured by the Coriolis meter transmitter is directly proportional to the mass flow rate of the fuel, CNG in this case. Since CNG is stored at a very high pressure, a pressure reducer is used to reduce the pressure and bring the gas pressure down to atmospheric pressure. Reduced pressure fuel line was connected just ahead of throttle in the air intake system in order to prepare fuel-air mixture.

A capacitance discharge ignition system (Altronic Inc., USA; CD200) was installed and used as a conventional spark ignition system. This system consists of a control unit, magnetic pickup sensor, input-output harness, timing disc and an ignition coil. The system provides approximately 65 mJ

energy in every spark. The spark plug used in this investigation is J-type and is located centrally in the cylinder head (figure 1). Spark gap was approximately 0.65 mm. Spark timing can be retarded upto 25 crank angle degrees.

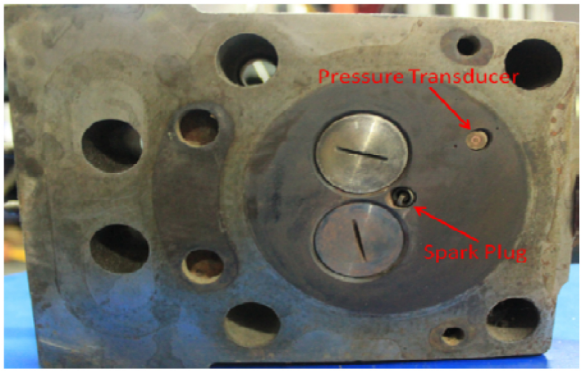

Figure 1. Location of spark plug in the cylinder head

For the LI, a laser spark plug was also designed and manufactured (figure 2). Laser spark plug was installed in the cylinder head in place of the conventional spark plug. Laser spark plug consists of two parts; a window holder and a lens holder. Window holder was first tightened into the cylinder head. Then the lens holder was screwed into the window holder. Focusing lens cannot withstand harsh conditions prevailing at the time of combustion having extreme pressures and temperatures. Therefore, a sapphire window (thickness 3 mm; diameter 12.5 mm) was used to seal the combustion gases from leaking out and damaging the lens.

Figure 2. Laser spark plug

Location of plasma inside the combustion chamber can be moved up and down by rotating the lens holder inside the window holder. One rotation of lens holder moves the plasma position by approximately 1 mm. This way, plasma position inside the combustion chamber can be changed using the same lens.

A flash lamp pumped Q-switched (Q-switching is a way of obtaining short, powerful pulses of laser radiation) Nd: YAG laser (Litron, UK; Nano L-200-30) delivering pulse energies upto 200 mJ with a pulse duration of 6-9 ns at full width half maximum (FWHM) at the fundamental wavelength (1064 nm) was used in this study. Laser beam diameter was 5 mm ($1/e^2$). Maximum internal repetition rate of laser was 30 Hz. Beam quality of the laser (M^2 value) was 7.3. M^2 value is a very important parameter in LI. An aperture of 2.9 mm diameter was inserted between the safety shutter and output mirror of the laser to enhance the beam quality and reduce the M^2 value. This however leads to reduction in maximum pulse energy. Laser pulse energy could be attenuated continuously by an external wave plate/ polarizer setup without affecting any other laser parameters such as pulse duration or spatial beam profile. The energy of each pulse was measured using a pyroelectric detector (Coherent, UK) and a laser energy meter (Coherent, UK). Pulse to pulse energy variation was measured and was found to be ±0.2 mJ. Plasma formation through laser spark plug in the atmosphere (outside the engine) is shown in figure 3.

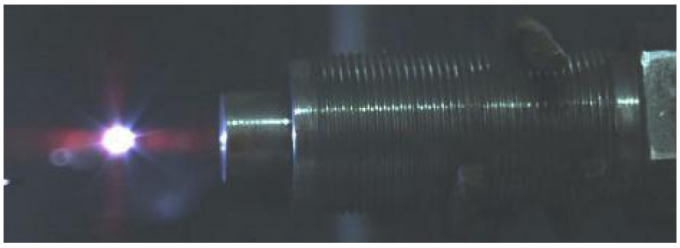

Figure 3. Plasma formation in atmosphere using laser spark plug. Laser beam is coming from right to the left.

Laser beam propagated in open atmosphere from laser head to the laser spark plug in the engine experiments. The laser beam was first passed through a diverging and collimating unit, where it gets enlarged to a parallel beam of larger diameter. This beam then gets reflected by a reflector into the Laser Spark plug. Optical beam path is shown in figure 4.

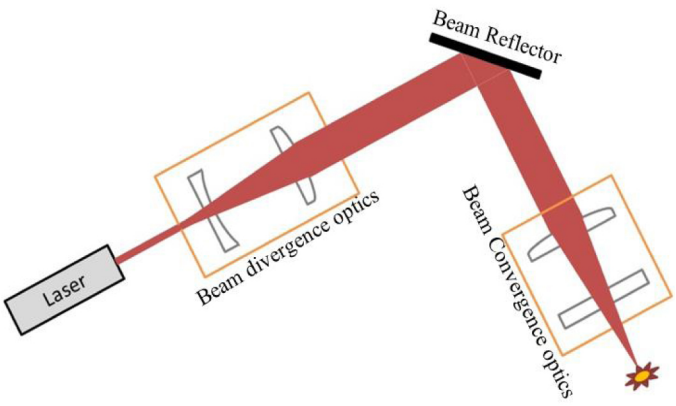

Figure 4. Optical beam path for the engine experiment

An electronic circuit was designed and developed to trigger the laser at the specified crank angle position i.e., at a certain ignition timing. This circuit requires 5 V DC power supply. Encoder and TDC signals were given to the electronic circuit. An encoder with a resolution of 0.5° CA was installed onto the crank shaft. Therefore, in a complete engine cycle, encoder generates 1440 TTL pulses. TDC sensor was installed on the camshaft such that in each engine cycle, one TTL pulse is generated. A microcontroller was programmed to perform the triggering. It starts to count the number of encoder pulses as soon as TDC pulse becomes high. Number of counts were fixed for any specified ignition timing. When the number of counts is equal to the fixed value, microcontroller generates a square pulse and the counter is reset to zero until the next TDC pulse becomes high. Electronic pulse diagram is shown in figure 5. This output pulse is used to trigger the laser. Laser is kept in external trigger mode therefore as soon as it receives the trigger pulse, a laser pulse is fired. Number of counts can be changed by microcontroller programming for different ignition timings.

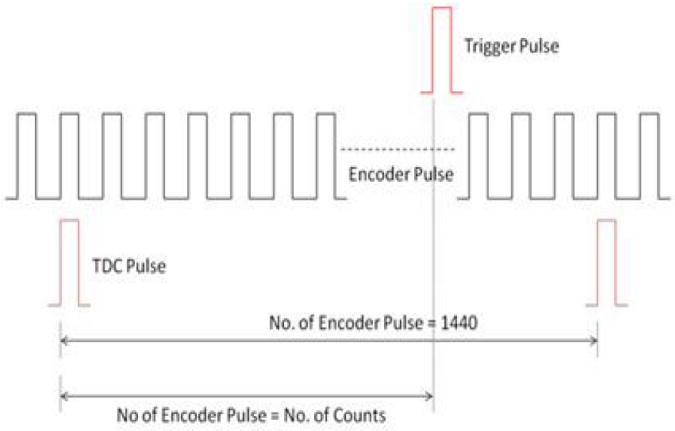

Figure 5. TTL pulse diagram

For the measurement of In-cylinder pressure, a piezoelectric pressure transducer (Kistler, Switzerland; 6013C) was installed in the cylinder head. Pressure signals were acquired w.r.t. crank angle signals from a precision shaft encoder (Encoders India; ENC58/6-720AB), which is installed onto the engine crankshaft. The charge produced by the pressure transducer is converted into proportional voltage signal by a charge amplifier (Kistler, Switzerland; 5015). The signal from charge amplifier is acquired by a high speed combustion data acquisition system (HI-Technique, USA; meDAQ), which digitizes and stores the signals for suitable post processing and analysis.

Concentrations of gaseous emissions such as HC, NO_x, CO, and CO_2 in the engine exhaust were measured using raw exhaust gas emission analyzer (Horiba, Japan; EXSA-1500). NO_x emissions were measured using Chemiluminescence emission analyzer, while CO and CO_2 were measured by infrared emission analyzer. Total hydrocarbons were measured using hot flame ionization detector. Experiments were carried out at constant engine speed (1500 rev/min) and wide open throttle conditions. Schematic of the experimental set up is shown in figure 6. Results were compared for conventional SI and LI. Plasma location inside the engine combustion chamber was varied for LI and engine performance, combustion, and emissions behavior were compared.

RESULTS AND DISCUSSION

In the LI system, a lens of 50 mm focal length was used to focus the laser beam. Plasma location was kept at same location inside the cylinder for both ignition systems. Laser pulse energy was measured outside the engine keeping the optical beam path same as the engine experiments. 15 mJ/ pulse laser energy was used for all engine operating conditions. Laser and conventional spark, both were fired at 250 CA before top dead centre (BTDC). 250 CA BTDC was the maximum break torque (MBT) position for conventional SI system.

Figure 7 shows the in-cylinder pressure and rate of heat release variation for laser and conventional spark w.r.t. crank angle position. In-cylinder pressure and heat release curves are in the figure are an average of 100 consecutive engine cycles. This is done in order to reduce the effect of cyclic variations.

It can be seen from the figure 7 that LI gives slightly higher in-cylinder pressure as well as advanced start of pressure rise and heat release compared to conventional SI at identical engine operating conditions. Biruduganti et al. [25] and Bihari et al. [27] also reported higher rate of pressure rise with LI compared to SI. Higher rate of pressure rise and rate of heat release validates the assertion about the possible use of LI for lean burn applications. However in-cylinder pressure variation remains almost same at λ = 1.05, 1.0 and 0.9.

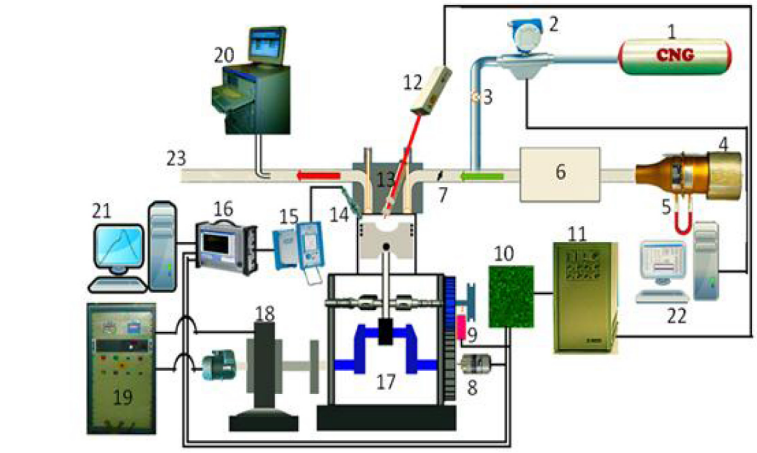

Figure 6. Schematic of experimental set-up 1. CNG cylinder, 2. CNG mass flow meter, 3. Flow control valve, 4. Laminar flow element, 5. U tube manometer, 6. Air box, 7. Throttle, 8. Shaft encoder, 9. TDC sensor, 10. Laser triggering circuit, 11. Laser power supply, 12. Nd: YAG laser, 13. Laser spark plug, 14. Pressure transducer, 15. Charge amplifier, 16. Data acquisition system, 17. Single cylinder engine, 18. Dynamometer, 19. Dyno controller, 20. Raw exhaust gas emission analyzer, 21. Data acquisition computer, 22. Computer for control of ignition and CNG flow meter, 23. Exhaust manifold.

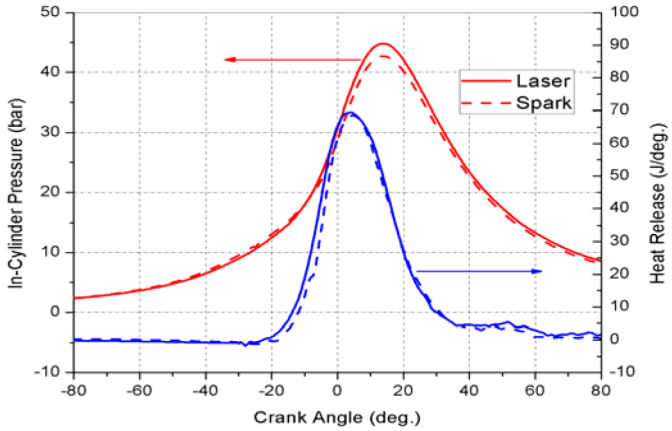

Figure 7. Comparison of in-cylinder pressure and heat release rate for LI and SI for WOT at 1500 rev/min, λ = 1.2

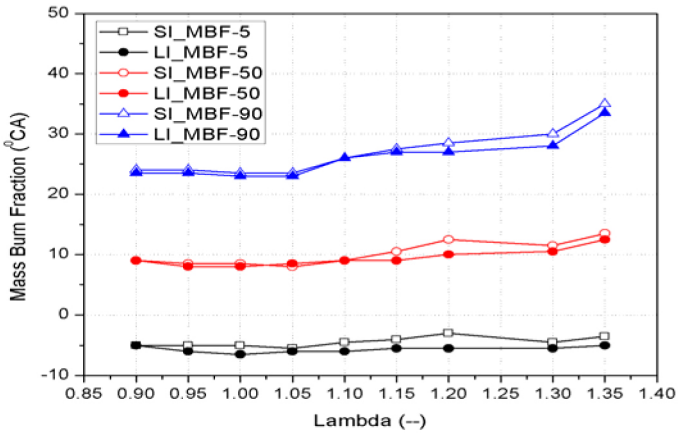

Figure 8. Comparative variation of 5%, 50% and 90% MBF for SI and LI with λ for WOT at 1500 rev/min

Different stages of combustion were calculated from mass burn fraction (MBF) curves. Figure 8 shows the variation of different stages of combustion for SI and LI. In the figure 8, 5%, 50%, and 90% MBF are presented. It can be seen from the figure that combustion starts earlier in LI as compared to SI for all values of λ. Combustion start earlier in LI by roughly 0.5-3.00 CA compared to SI at different mixture strengths. Ignition delay, which is defined as the crank angle interval between spark discharge and 5% MBF, was also found to be lower in case of LI compared to SI because of this earlier start of combustion for the same ignition timing at the same mixture strength. Also, because of the absence of any electrodes close to the plasma (as is the case in conventional SI, where these electrodes act as spark energy sink), all spark energy is utilized in initiating the flame kernel, leading to faster initial combustion and higher heat release rates.

Cycle-to-cycle variations in SI engine are a limiting factor in engine performance, fuel economy and emissions. Variations in combustion leads to varying work output per cycle, which translates into fluctuations in the engine speed, and torque, thus directly affecting vehicle drivability adversely. Cyclic variations pose a major problem in lean burn SI engine. Therefore cycle-to-cycle variations were investigated for SI and LI. Cycle-to-cycle variations are characterized by the coefficient of variation (COV) of indicated mean effective pressure (IMEP). Figure 9 shows the relative variation of COV of IMEP for SI and LI with varying λ.

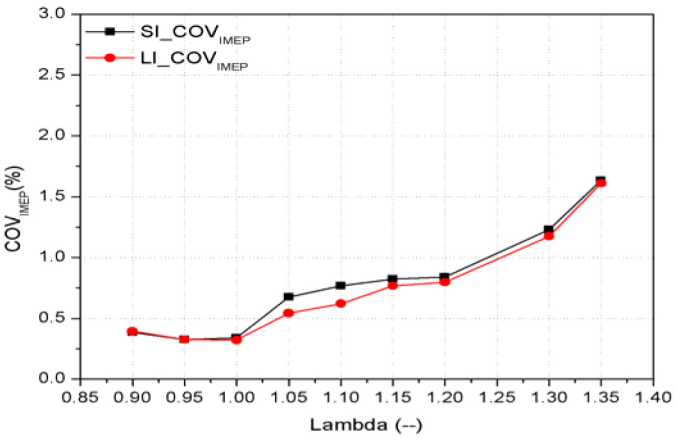

Figure 9. Comparative variation of COVIMEP for SI and LI with λ for WOT at 1500 rev/min

It can be noted from figure 9 that COV_{IMEP} increases as λ decreases/ decreases from the stoichiometric mixture and is minimum for stoichiometric mixtures. COV_{IMEP} is found to be relatively lower for LI compared to SI for all lean engine operating conditions. This indicates that the combustion stability of LI is superior to conventional SI. Cycle-to-cycle variation in SI engine is influenced by the variations in the early stages of combustion. Any factor which increases the flame speed, will lead to reduction in cycle-to-cycle variations [35, 36]. Flame speed with LI would be higher compared to SI at the same operating conditions of the engine because of absence of flame quenching and higher rate of energy deposition/ energy absorption in the laser plasma. Therefore lower COV is observed in LI compared to SI. However COV_{IMEP} was seen to be almost same for LI and SI for the richer mixtures.

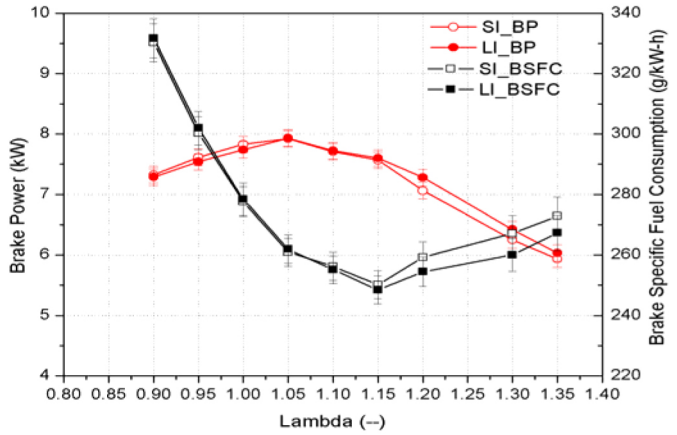

Figure 10. Comparative variation of BSFC and brake power for SI and LI with λ for WOT at 1500 rev/min

After combustion characterization, engine performance parameters such as brake power and brake specific fuel consumption (BSFC) of the engine are compared for SI and LI. It can be seen from figure 10 that brake power increases with decreasing λ and reaches a maxima, and then decreases with further reduction in λ. At very high λ i.e. leaner mixtures, combustion is limited because of availability of very small fuel quantity and at lower λ i.e. for richer mixtures, combustion is limited because of the limited availability of air for combustion in the cylinder. Because of these two limiting factors, brake power first increases as λ decreases and then decreases with further reduction in λ. Brake power is also observed to be marginally higher for LI compared to SI in figure 10. This may be attributed to more efficient combustion observed in LI compared to SI (Figure 7). BSFC is observed to be decrease as λ decreases and reaches at a minima before increasing again with further reduction in λ, i.e. with mixture enrichment. Lower BSFC is seen in case of LI compared to SI upto λ = 1.15. Mixtures richer than λ = 1.15 give almost same BSFC for SI as well as LI.

Engine exhaust emissions were also compared for SI and LI. Figure 11 shows the variation of brake specific NOx (BSNOx) and brake specific total hydrocarbon (BSTHC) emissions for SI and LI with varying λ. NOx formation inside the combustion chamber is highly dependent on the peak temperatures of the burned gas behind the flame front, where nitrogen available in the cylinder oxidizes to form oxides of nitrogen, and availability of excess oxygen. The highest burnt gas temperatures are obtained for mixture close to stoichiometric ratio, however there is hardly any excess oxygen available. As mixture becomes leaner, availability of excess oxygen/air in the cylinder increases, and the peak temperatures are still high, which give rise to formation of high amount of NOx. Because of this reason, maximum BSNOx is observed at intermediate value of λ = 1.15. BSNOx emissions were observed to be higher for LI compared to SI upto λ = 1.2. Further reduction in λ, BSNOx emission is observed to be almost similar for SI and LI. Higher BSNOx emission with LI are because of earlier start of combustion (Figure 8).

BSTHC emissions decrease with reduction in λ (upto 1.15) and reach a minima before increasing again with further reduction in λ beyond 1.15 for both SI and LI. BSTHC emissions are slightly lower for LI compared to SI combustion because of more efficient combustion at higher in-cylinder pressure (Figure 7).

After comparing LI and SI system performance, plasma location inside the engine cylinder was varied and its effect on the engine performance, combustion and emissions was investigated. Flexibility in plasma location inside the engine cylinder is an important advantage of the LI system. Figure 12 shows the variation of plasma location inside the engine cylinder (along red line). Due to mechanical constraints associated with installation of laser spark plug in the cylinder head, it was not possible to move the plasma along the cylinder axis and it could be moved along an axis, which was

inclined by 350 along with the engine cylinder axis (Figure 12).

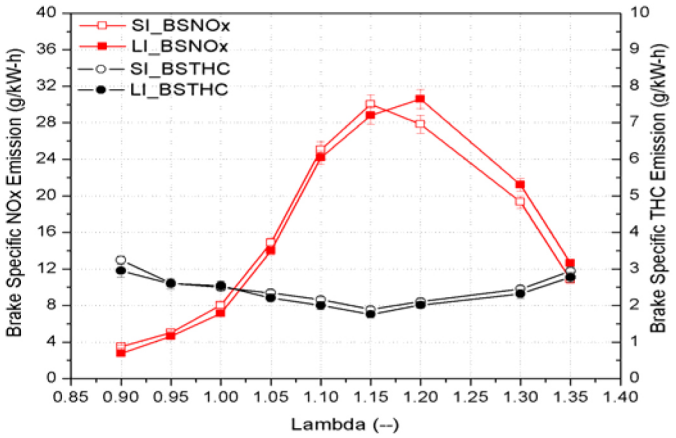

Figure 11. Comparative variation of BSNOx and BSTHC emissions for SI and LI with λ for WOT at 1500 rev/min

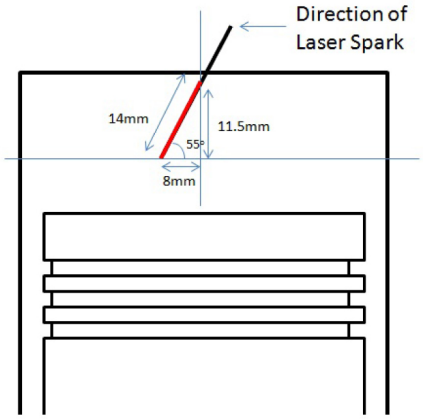

Figure 12. Variation of plasma location inside the engine cylinder

Plasma location could be moved by upto 14 mm inside the combustion chamber along the red line (figure 12) beginning with the location of conventional spark plug generated plasma location (considered base position; 0 mm). The experiments were performed by choosing the plasma location spots in steps of 2 mm along this axis.

Figure 13 shows the brake thermal efficiency (BTE), brake mean effective pressure (BMEP) and BSFC with variation in plasma location inside the engine cylinder. A marginal increase in BMEP was observed when the plasma location was changed from 0 to 6 mm inside the combustion chamber. However on further moving the plasma location inside the combustion chamber, a marked reduction in BMEP and thermal efficiency was observed. This effect was more clearly observed in BSFC curve, which showed a minima at 6 mm plasma position. BSFC reduced by 0.5% with LI at 6 mm plasma position compared to SI at 0 mm position while BTE increased by approximately 0.5% for the same.

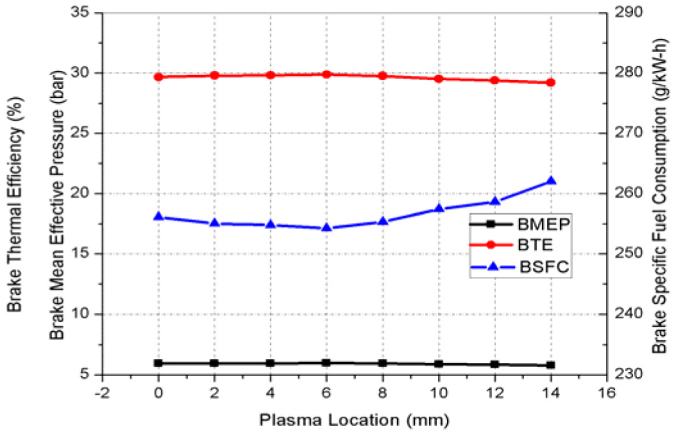

Figure 13. Performance of engine with variation of plasma location inside the engine cylinder for WOT at 1500 rev/min, λ = 1.2

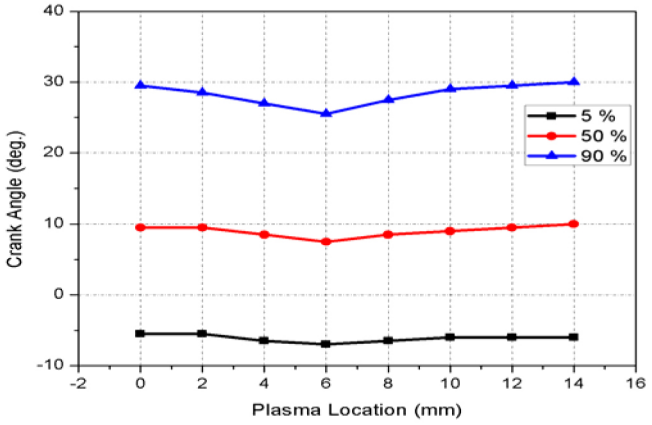

Figure 14. MBF CAD with variation of plasma location inside the cylinder for WOT at 1500 rev/min, λ = 1.2

Figure 14 shows the crank angle position, at which 5%, 50% and 90% MBF occurs with the variation in plasma position. 5% MBF is generally regarded as the start of combustion; and 90% MBF is considered as the end of combustion and the difference between the two as combustion duration. Combustion started at 5.5° CA BTDC, when the plasma position was at the conventional spark plug location whereas combustion stared relatively earlier (7.0° CA BTDC), when LI plasma position moved inside the cylinder by 6 mm. Thus ignition delay is shortened by 1.5° CA. With conventional SI, combustion started at 3.0° CA BTDC. 90% MBF decreases as the LI plasma position shifts from conventional spark location to 6 mm position. After that, the 90% MBF position advances with further downward movement of plasma. 90% MBF position retards by 4.0° CA as plasma position was moved from conventional spark position to 6 mm downward along the axis. This is possibly because of reduction in maximum flame propagation distance and moving the flame

kernel away from the metallic surfaces, which reduces the heat loss and promotes faster early flame kernel growth.

Ahrens et al. [37] performed LI experiments and changed the plasma locations to four different positions inside the engine cylinder. They reported that plasma location slightly offset from the cylinder geometry centre towards the intake valve was the most optimum location in terms of MBF and combustion stability. Graf et al. [38] also investigated the plasma location variation in a single cylinder direct injection gasoline engine and reported that combustion duration shortens with movement of plasma location inside the cylinder albeit upto a certain depth (12 mm). Thereafter it starts to increase again.

Variation of brake specific mass emissions with plasma position is shown in figure 15. BSCO2 emissions were almost constant for the entire range of plasma position variation. BSCO and BSTHC remain constant upto 6 mm and then start to increase. Slightly higher BSNOx emissions were observed at 6 mm plasma position compared to conventional spark location. Higher BSNOx emissions are attributed to faster combustion and higher heat release rate at this location.

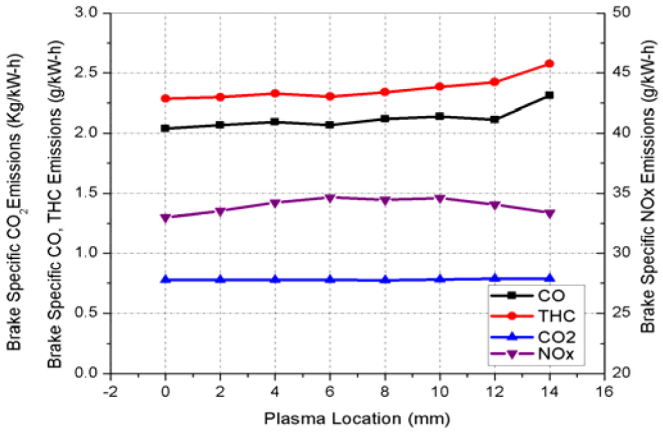

Figure 15. BSCO, $BSCO_2$, BSTHC and BSNOx emission with variation of plasma location inside the cylinder for WOT at 1500 rev/min, λ = 1.2

CONCLUSIONS

Laser ignition (LI) of CNG air mixtures was carried out on a single cylinder engine at constant speed (1500 rev/min) and wide open throttle and it was compared with conventional spark ignition (SI). With LI, high peak in-cylinder pressures, earlier start of pressure rise and higher heat release rates were observed in comparison to conventional spark plug system operating under identical engine operating conditions. Combustion starts earlier for LI by 0.5-3.0° CA compared to SI for different mixture strengths. Brake power output was observed to be marginally higher for LI compared to SI. Lower BSFC was seen for LI compared to SI λ = 1.15, after which BSFC was almost similar for both cases. BSNOx emissions were observed to be higher for LI compared to SI upto λ = 1.2. Upon further reduction in λ, BSNOx emissions were observed to be almost same. BSTHC emissions were also slightly lower for LI compared to SI because of more efficient combustion for LI. Laser plasma location was varied upto 14 mm depth inside the cylinder and engine performance, combustion and emissions were investigated for varying plasma locations. A marginal increase in brake power output and brake specific fuel consumption were observed, when plasma position was varied from conventional spark location to 6 mm. Slightly higher BSNOx emissions were observed at the 6 mm plasma position.

REFERENCES

1. Weinrotter, M., Kopecek, H., and Wintner, E., "Laser Ignition of Engines," Laser Physics, 15(7): 947-953, 2005.

2. Phuoc, T.X., Single-Point Verse Multi-Point Laser Ignition: Experimental Measurements of Combustion Times and Pressures," Combustion and Flame, 122(4): 508-510, 2000, doi: 10.1016/S0010-2180(00)00137-1.

3. Morsy, M.H., Ko, Y.S., Chung, S.H., and Cho, P., "Laser-Induced Two Point Ignition of Premixed with a Single Shot Laser," Combustion and Flame, 124(4): 724-727, 2001, doi: 10.1016/S0010-2180(00)00218-2.

4. Maker, P.D., Terhune, R.W., and Savage, C.M., "Optical Third Harmonic Generation," Proceedings of Third International Conference on Quantum Electronics, Paris, Columbia University Press, New York, 2: 1559, 1964.

5. Damon, E., and Thomlinson, R., "Observation of Ionization of Gases by a Ruby Laser," Applied Optics, 2(5): 546-547, 1963, doi: 10.1364/AO.2.000546.

6. Meyerand, R.G., and Haught, A.F., "Gas Breakdown at Optical Frequencies," Physical Review Letters, 11(9): 401-403, 1963, doi: 10.1103/PhysRevLett.11.401.

7. Minck, R.W., "Optical Frequency Electrical Discharges in Gases," Journal of Applied Physics, 35(1): 252-254, 1964, doi: 10.1063/1.1713085.

8. Phuoc, T.X., "Laser-Induced Spark Ignition Fundamental and Applications," Optics and Laser in Engineering, 44(5): 351-397, 2006, doi: 10.1016/j.optlaseng.2005.03.008.

9. Kopecek, H, Maier, H, Reider, G, Winter, F, and Wintner, E. "Laser Ignition of Methane-Air Mixtures at High Pressures," Experimental Thermal and Fluid Science, 27(4): 499-503, 2003, doi: 10.1016/S0894-1777(02)00253-4.

10. Phuoc T. X., "Laser Spark Ignition: Experimental Determination of Laser-Induced Breakdown Thersolds of Combustion Gases," Optics Communications, 175(4-6): 419-423, 2000, doi: 10.1016/S0030-4018(00)00488-0.

11. Phuoc, T.X., and White, F.P., "Laser-induced spark ignition of CH_4/air mixtures," Combustion and Flame,

199(3): 203-216, 1999, doi: 10.1016/S0010-2180(99)00051-6.

12. Radziemski, L.J., and Cremers, D.A., "Laser-Induced Plasmas and Application," New York-Basel, Marcel Dekker Inc., 1989.

13. Bekefi, G., "Principles of Laser Plasma," John Wiley and Sons Inc, 1976.

14. Tozer, B.A., "Theory of Ionization of Gases by Laser Beams," Physical. Review, 137(6A): A1665-A1667, 1965, doi: 10.1103/PhysRev.137.A1665.

15. Paul, D.R. "Laser versus Conventional Ignition of Flames," Optical Engineering, 33(2): 510-521, 1994, doi: 10.1117/12.152237.

16. Weinrotter, M., Kopecek, H., Wintner, E., Lackner, M., and Winter, F., "Application of Laser Ignition to Hydrogen-Air Mixtures at High Pressures," International Journal of Hydrogen Energy, 30(3) :319-326, 2005, doi: 10.1016/j.ijhydene.2004.03.040.

17. Forsich, C., Lackner, M., Winter, F., Kopecek, H., and Wintner, E., "Characterization of Laser-Induced Ignition of Biogas-Air Mixtures," Biomass and Bioenergy, 27(3): 299-312, 2004, doi: 10.1016/j.biombioe.2004.02.002.

18. Alocock, A.J., Kato, K., and Richardson, M.C., "New Features of Laser-Induced Gas Breakdown In The Ultraviolet," Optics Communication, 6(4): 342-344, 1972, doi: 10.1016/0030-4018(72)90151-4.

19. Dewhurst, R.J., "Comparative Data on Molecular Gas Breakdown Thresholds in High Laser-Radiation Fields," Journal of Physics D, Applied Physics, 11(16): L191-L195, 1978, doi: 10.1088/0022-3727/11/16/002.

20. Rosen, D.I., and Weyl, G., "Laser-Induced Breakdown in Nitrogen and the Rare Gases at 0.53 And 0.35μm," Journal of Physics D, Applied Physics, 20(10): 1264-1276, 1987, doi: 10.1088/0022-3727/20/10/009.

21. Bradley, D., Sheppard, C.G.W., Suardjaja, I.M., and Woolley, R., "Fundamentals of High-Energy Spark Ignition with Lasers," Combustion and Flame, 138(1-2): 55-77, 2004, doi: 10.1016/j.combustflame.2004.04.002.

22. Young, M., and Hercher, M., "Dynamics of Laser Induced Breakdown in Gases," Journal of Applied Physics, 38(11): 4393-4400, 1967, doi: 10.1063/1.1709137.

23. Herdin, G., Klausner, J., Wintner, E., Weinrotter, M., and Graf, J., "Laser Ignition - A New Concept to Use and Increase the Potential of Gas Engines," ICED ASME Technical Fall conference, Paper no. ICEF2005-1352, 2005, doi: 10.1115/ICEF2005-1352.

24. Dale, J., Smy, P., and Clements, R., "Laser Ignited Internal Combustion Engine - An Experimental Study," SAE Technical Paper 780329, 1978, doi: 10.4271/780329.

25. Biruduganti, M. S., Gupta, S. B., Bihari, B., Klett, G., and Sekar, R., "Performance Analysis of a Natural Gas Generator Using Laser Ignition," ICED ASME Technical Fall conference, Paper no. ICEF2004-983, 2004, doi: 10.1115/ICEF2004-0983.

26. Mcmillian, M.H., Woodruff, S.D., Richardson, S.W., and McIntyre, D., "Laser Spark Ignition: Laser Development and Engine Testing," ICED ASME Technical Fall conference, Paper No. ICEF2004-917, 2004, doi: 10.1115/ICEF2004-0917.

27. Bihari, B., Gupta, S. B., Sekar, R. R., Gingrich, J., and Smith, J., "Development of Advanced Laser Ignition System for Stationary Natural Gas Reciprocating Engines," ICED ASME Technical Fall conference, Paper no. ICEF2005-1325, 2005, doi: 10.1115/ICEF2005-1325.

28. Richardson, S.W., Mcmillian, M.H., Woodruff, S.D., Worstell, T., and McIntyre, D.L., "Laser Spark Ignition of a Blended Hydrogen-Natural Gas Fueled Single Cylinder Engine," ICED ASME Technical spring conference, Paper no. ICES2006-1397, 2006, doi: 10.1115/ICES2006-1397.

29. Liedl, G., Schuocker, D., Geringer, B., Graf, J., Klawatsch, D., Lenz, H.P., Piock, W.F., Jetzinger, M., and Kapus, P., "Laser Induced Ignition of Gasoline Direct Injection Engines," Proceeding of SPIE, 5777, 955-960, 2005, doi: 10.1117/12.611324.

30. McIntyre, D.L., Woodruff, S.D., McMillian, M.H., and Richardson, S.W., "Lean-Burn Stationary Natural Gas Reciprocating Engine Operation with a Prototype Miniature Diode Side Pumped Passively Q-Switched Laser Spark Plug," ICED ASME Technical spring conference, Paper no. ICES2008-1696, 2008, doi: 10.1115/ICES2008-1696.

31. Kroupa, G., Franz, G., and Winkelhofer, E., "Novel Miniaturized High-Energy Nd-YAG Laser for Spark Ignition in Internal Combustion Engines," Optical Engineering, 48(1): 014202-1-5, 2009, doi: 10.1117/1.3072958.

32. Yalin, A. P., Defoort, M. W., Joshi, S., Olsen, D., and Willson, B., "Laser Ignition of Natural Gas Engines Using Fiber Delivery," ICED ASME Technical Fall conference, Paper no. ICEF2005-1336, 2005, doi: 10.1115/ICEF2005-1336.

33. Tauer, J., Kofler, H., Schwarz, E., and Wintner, E., "Transportation of Megawatt Millijoule Laser Pulse Via Optical Fibers?," Central European Journal of Physics, 8(2): 242-248, 2010, doi: 10.2478/s11534-009-0146-1.

34. Stakhiv, A., Gilber, R., Kopecek, H., Zheltikov, A.M., and Wintner, E., "Laser Ignition of Engines via Optical Fibers?," laser Physics, 14(5): 738-747, 2004.

35. Ishii, K., Sasaki, T., Urata, Y., Yoshida, K. et al., "Investigation of Cyclic Variation of IMEP Under Lean Burn Operation in Spark-Ignition Engine," SAE Technical Paper 972830, 1997, doi: 10.4271/972830.

36. Zervas, E., "Correlations Between Cycle-to-Cycle Variations and Combustion Parameters of a Spark Ignition

Engine", Applied Thermal Engineering, 24: 2073-2081,2004, doi: 10.1016/j.applthermaleng.2004.02.008.

37. Ahrens, D.L., Olsen, D.B., and Yalin, A.P., "Development of an Open Path Laser Ignition for a Large Bore Natural Gas Engine: Part 2 Single Cylinder demonstration," ICED ASME Technical Fall conference, Paper no. ICEF2005-1317, 2005, doi: 10.1115/ICEF2005-1317.

38. Graf, J., Weinrotter, M., Kopecek H., and Wintner, E., "laser Ignition, Optics, and Contaminations of Optics in an I.C. Engine," ICED ASME Technical Fall conference, Paper No. ICEF 2004-833, 2004, doi: 10.1115/ICEF2004-0833.

ACKNOWLEDGEMENTS

The authors would like to acknowledge the grant from SERC, Department of Science and Technology, Government of India for carrying out this investigation (Grant No. SR/S3/MERC/0068/2008). The authors would also like to acknowledge CSIR, for offering the Pool Scientist Position to Mr. Dhananjay Kumar Srivastava to work in ERL and complete this task. Mr. Kewal Dharmashi, Graduate student in ERL helped in carrying out the experiments along with Mr. Roshan and Mr. Ravi.

DEFINITIONS/ABBREVIATIONS

λ - Relative air-fuel ratio

M^2 - Beam quality factor

BTDC - Before top dead centre

BSCO - Brake specific carbon mono-oxide

BSFC - Brake specific fuel consumption

BSTHC - Brake specific total hydrocarbon

IB - Bremsstralhung collisions

COV - Coefficient of variation

CNG - Compressed natural gas

CR - Compression ratio

CA - Crank angle

FWHM - Full width half maximum

IMEP - Indicated mean effective pressure

LFE - Laminar flow element

LI - Laser ignition

MBF - Mass burn fraction

MBT - Maximum brake torque

MPI - Multi-photon ionization

SI - Spark ignition

TDC - Top dead centre

TTL - Transistor-transistor logic

WOT - Wide open throttle

The Engineering Meetings Board has approved this paper for publication. It has successfully completed SAE's peer review process under the supervision of the session organizer. This process requires a minimum of three (3) reviews by industry experts.

ISSN 0148-7191

SAE Customer Service:
Tel: 877-606-7323 (inside USA and Canada)
Tel: 724-776-4970 (outside USA)
Fax: 724-776-0790
Email: CustomerService@sae.org
SAE Web Address: http://www.sae.org
Printed in USA